JOC The Journal of Organic Chemistry
Cite This: J. Org. Chem. 2019, 84, 8759−8765
Note
pubs.acs.org/joc

Modulation of Reduction Potentials of Bis(pyridinium)alkane Dications through Encapsulation within Cucurbit[7]uril

Nikolai A. Tcyrulnikov,[†] Ramkumar Varadharajan,[‡] Anastasiia A. Tikhomirova,[†] Mahesh Pattabiraman,*[,§] Vaidhyanathan Ramamurthy,*[,‡] and R. Marshall Wilson*[,†]

[†]Center for Photochemical Sciences and Chemistry Department, Bowling Green State University, Bowling Green, Ohio 43403, United States

[‡]Department of Chemistry, University of Miami, Coral Gables, Florida 33146, United States

[§]Department of Chemistry, University of Nebraska, Kearney, Nebraska 68849, United States

Supporting Information

ABSTRACT: Supramolecular modulation of reduction potentials of two series of bis(pyridinium)alkane salts is described. Study of the encapsulation of bis(pyridinium)alkane guests within the CB[7] cavity revealed the critical influence of the linker length and the position of the heteroatom on the reduction potentials of encapsulated guests. CB[7] complexation of pyridinium salts induced reduction potential changes ranging between +50 and −430 mV. Noncovalent modulation of the electron-accepting ability of organic cations can be utilized in electron-transfer-initiated reactions.

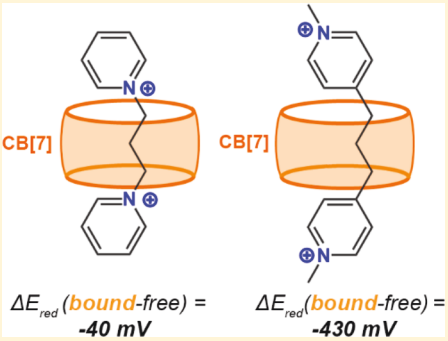

Cucurbit[n]urils (CB[n], n = 5−10) are a family of macrocyclic molecular containers containing two polar carbonyl hydrophilic portals decorating the relatively hydrophobic inner cavity.[1−3] These features are responsible for the unique binding properties and widespread use of CBs in self-assembly,[4,5] molecular recognition,[6−8] catalysis,[9−11] drug delivery,[12,13] and design of molecular machines.[14,15] Since the reports by Kaifer[16] and Kim[17] describing CB[7] encapsulation of redox active methyl viologens (MV^{2+}) there has been significant interest in using CBs to modulate physicochemical properties of MVs.[18−21] However, to our knowledge, there is no comprehensive study correlating redox behavior with the structural features of the redox-active guests included within CB. Information on the ability of CBs to manipulate electron-transfer processes would expand the utility of CBs in the aforementioned areas. Binding of various *N*-heterocyclic cations was studied by Macartney and co-workers.[22−24] They suggested that for most of the species, pyridinium nitrogen resides adjacent to the polar carbonyl portals, while a hydrophobic linker is included within the CB[7] cavity. These electron-acceptor compounds are of interest not only as photo- and electro- chemically induced electron delocalizing molecules[25] but also as antimicrobial agents.[26,27] In this work, we studied two series of bis-(pyridinium)alkane guests (Figure 1). We have demonstrated that CB[7] encapsulation and favorable ion−dipole interaction between pyridinium nitrogens and carbonyl rims influences the reduction potentials of bis(pyridinium)alkane dications. The results of this study highlight that although the irreversibility of

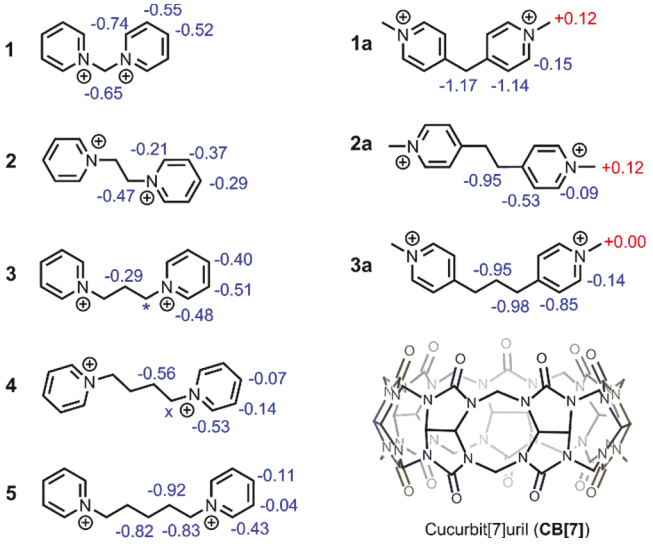

Figure 1. CB[7] complexation induced ^{1}H NMR chemical shifts (CIS, ppm) of bis(pyridinium)alkane guests; maximum CIS values from titration to up to 4:1 host−guest ratio are shown (for details, see the SI); blue, upfield shift; red, downfield shift; *, merged with H_2O; x, merged with CB[7].

Received: April 16, 2019
Published: June 12, 2019

DOI: 10.1021/acs.joc.9b01049
J. Org. Chem. 2019, 84, 8759−8765

the reduction cannot be altered, the reduction potentials of bis(pyridinium)alkanes in aqueous media can be supramolecularly varied over a wide range (between +50 and −430 mV) and that slight structural variations in the length of the linker and the position of *N*-atom can impart significant changes in redox properties of bis(pyridinium)alkane CB[7] complexes. Recently, we reported the oxidation of **1a** under aerobic conditions.[28] This effect is noticeable only upon prolonged exposure and did not affect the measurements in this work.

We have employed ^{1}H NMR to infer the inclusion of guests within the CB[7] cavity.[23,29] Hydrogens of guests located within the hydrophobic cavity of CB[*n*] typically exhibit an upfield shift ($\Delta\delta_{\text{comp-free}} < 0$), and those remaining adjacent to carbonyl portals display a zero or downfield shift ($\Delta\delta_{\text{comp-free}} > 0$). Figures 2 and 3 reveal that the inclusion of **1** and **5** within

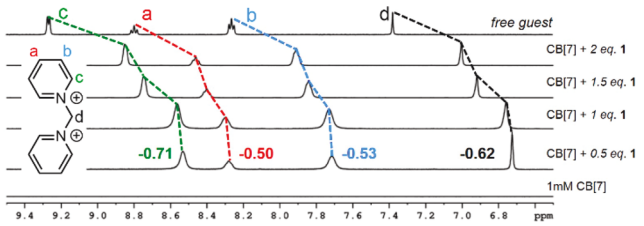

Figure 2. Variation in ^{1}H chemical shifts for titration of 1 mM CB[7] with 30 mM **1** in D_2O: top spectrum, free guest; bottom spectrum, free host.

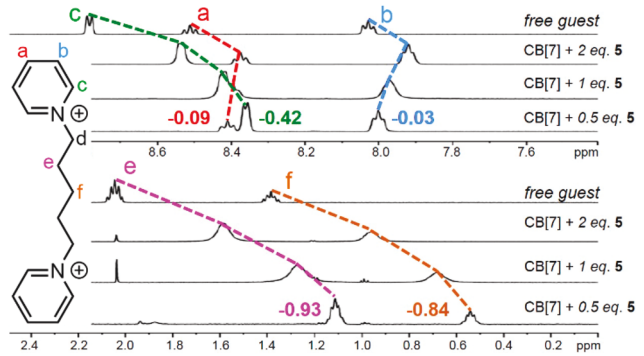

Figure 3. Complexation-induced shifts in ^{1}H NMR signals of **5** upon addition to CB[7] (1 mM) in D_2O. Aromatic (top) and aliphatic (bottom) regions of the spectra are presented.

CB[7] results in the upfield shift of both methylene and aromatic protons. Neither broadening of the signals nor separate resonances were observed, indicating that CB[7] is sliding fast over both alkyl chain and aromatic rings in the NMR time scale.[22] Similar features were noted for **2**−**4** (Figures S4, S7, and S11).

^{1}H NMR titration experiments confirmed that **1**−**5** formed a 1:1 complex (Figures S3, S6, S10, S14, and S18). Of the five guests, **1**−**3** experienced upfield shifts in the range from −0.3 to −0.6 ppm for aliphatic and from −0.2 to −0.7 ppm for aromatic protons. Latter values are much greater than the ones experienced by **4** and **5**. In fact, *para* and *meta* protons (a and b) of **4** and **5** showed only a small shift (Figure 3). We believe the small shifts indicate the proximity of the aromatic rings to the carbonyl portals.

The length and hydrophobicity of the methylene chain suggest that it would prefer the interior of the CB[7] to the hydrophilic rim. Consistent with this, aliphatic protons of **4** and **5** experience the largest upfield shifts in the series, indicating that CB[7] slides over alkyl chains in both molecules. Unlike **1**−**4**, **5** showed binding induced NMR changes in the presence of excess CB[7], suggesting the formation of the 2:1 host−guest complex and fast exchange between the 1:1 and 2:1 complex (in this paper, the ratio is presented as host to guest).[22] The reversal in direction of CIS (signal a, Figure 3) for **5** beyond 1 equiv of CB[7] and its saturation beyond 2 equiv suggests the ability of **5** to form a higher order complex in a stepwise equilibrium. This could be attributed to the optimal concentration (mM) of the host and guest in the solution and the length of the pentylene linker, which allows simultaneous binding to two CB[7] without significant steric hindrance between them.

Host−guest structures inferred from the ^{1}H NMR data are in line with the computationally generated structures optimized at the HF/3-21G level (Figure 4, Figures S85−

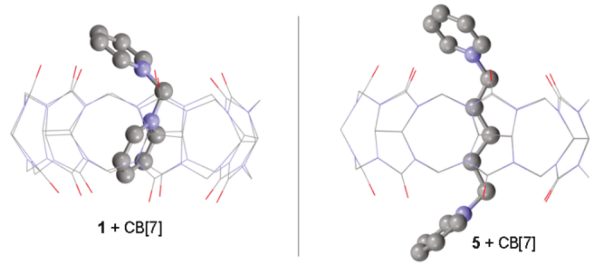

Figure 4. Computationally generated structures of 1:1 complexes of **1** and **5** with CB[7].

S87). As expected, guests **1**−**3** in their extended conformations were mostly encapsulated within the CB[7] cavity. In the case of **5**, the predicted structure shown in Figure 4 is consistent with the NMR data. In this case, the aromatic rings are extended well outside the portals of CB[7].

Guests **1a**−**3a** exhibited behavior different from that of **1**−**5** in the presence of CB[7]. Two independent ^{1}H NMR signals for free and bound guests indicated a slow or lack of chemical exchange (in the NMR time scale) between these two types of guests. Compounds **1a**−**3a** displayed much larger upfield shifts for the methylene protons than **1**−**5** and a downfield shift of the methyl protons. ^{1}H NMR titration experiments confirmed the formation of 1:1 complexes.

To ascertain the host to guest ratio and to estimate the thermodynamic parameters of binding, the isothermal calorimetric measurements (ITC) were performed (Table 1).

Table 1 reveals that the host−guest ratio (*n*) in all cases is one which is consistent with NMR titration results. Except for **2**, all other guests exhibited a trend in their ΔH and ΔS values. Guests **1**, **3**, and **4** have a lower (−) ΔH and higher (+) ΔS than **1a**−**3a**. These results suggest that **1a**−**3a** are bound more tightly than **1**, **3**, and **4**. Clearly, the presence of two independent peaks in the NMR spectrum and the larger influence of CB[7] on the reduction potentials of **1a**−**3a** (see later section) must be a consequence of the stronger binding of these guests to CB[7].

Next, we proceeded to examine the influence of CB[7] on the electrochemical properties of **1**−**5** and **1a**−**3a**. The absence of the reverse oxidation wave or its large separation from the reduction peaks and dependence of the reduction potential on the scan rate confirmed the irreversibility of the electro-

DOI: 10.1021/acs.joc.9b01049
J. Org. Chem. 2019, 84, 8759−8765

Table 1. Binding Constant (K_a), Molar Ratio (n), Enthalpy (ΔH), and Entropy (ΔS) for Compounds 1−5 and 1a−3a with CB[7] at 25 °C Measured by ITC

	K_a[a] × 10^6 M^{-1}	n	ΔH (kJ/mol)	ΔS (J/mol·K)
1	1.53 ± 0.02	1.11 ± 0.01	−16.66 ± 0.08	62.54 ± 0.18
2	0.95 ± 0.09	1.16 ± 0.01	−27.01 ± 0.41	23.81 ± 0.54
3	3.17 ± 0.17	0.93 ± 0.02	−21.60 ± 0.15	52.02 ± 0.03
4	3.06 ± 0.53	0.97 ± 0.06	−19.03 ± 0.62	60.22 ± 0.64
1a	1.19 ± 0.15	0.91 ± 0.00	−29.21 ± 0.11	18.32 ± 0.69
2a	3.86 ± 0.06	0.98 ± 0.04	−27.57 ± 0.10	33.63 ± 0.21
3a	2.54 ± 0.01	1.04 ± 0.05	−29.64 ± 0.33	23.41 ± 0.80

[a]Mean value measured from two isothermal titration calorimetry experiments at 25 °C in DI water. We could not obtain reliable binding characteristics for **5**, possibly due its ability to form a higher order complex in addition to 1:1 complex.

chemical reduction of **1**−**5** and **1a**−**3a** (Figure 5C).[30] This is consistent with the irreversibility of *N*-methylpyridinium and

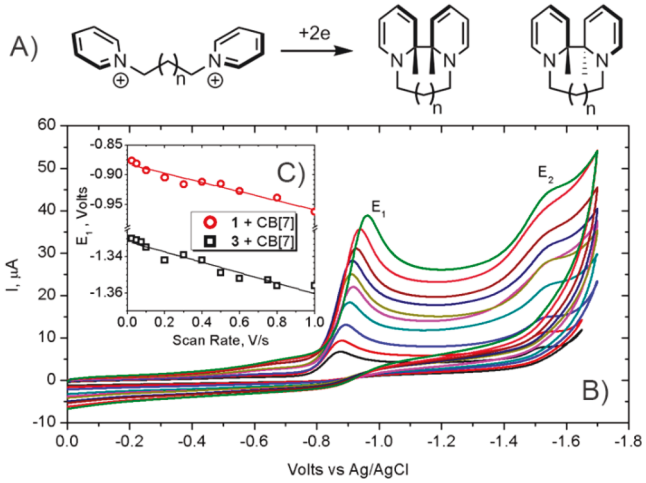

Figure 5. Irreversible electrochemical reduction (A); reduction of a 1:1 complex of **1** with CB[7] at different scan rates (B); reduction potentials of **1** (E_1) and **3** in the presence of CB[7] vs the scan rate.

bis(pyridinium)alkanes reduction leading to 4,4′-coupled σ-dimers and cyclomers, correspondingly (Figure 5, A).[31−34] Interestingly, irreversibility is not affected by CB[7], suggesting that cyclomerization and/or σ-dimerization is not prevented by inclusion within CB[7]. This is likely the result of neutral diradical intermediates, generated upon two-electron reduction, exiting the CB[7] host. Thus, we believe that the cyclomerization occurs outside the CB[7] host.[35]

Molecules listed in Figure 1 could undergo either a single step or stepwise reduction. We believe that the stepwise reduction is favored when the radical cation formed upon one electron reduction can be delocalized over both rings.[36−38] For this to occur, face-to-face interaction is required, which is only possible in the cisoid conformation of a bispyridyl system. Figure 5B (E_1 and E_2) shows that in the case of **1** stepwise reduction is favored (Figure S46 for **1a**). In this case, the energetically favorable radical cation intermediate leads to a positive shift of the first reduction potential (compared to *N*-methylpyridinium (−1.45 V vs Ag/AgCl)).[39] According to quantum chemical (QC) calculations, CB[7] encapsulation favors the transoid conformation for the longer chain guests. In such a conformer, direct electronic communication between aromatic units would decrease resulting in their independent reduction at potentials close to that of *N*-methylpyridinium. This should favor a single reduction peak. This is the case for CB[7]-included **2** and **2a** and longer chain systems (Figures S40, S41, S44, S45, and S47−S50).

Figure 6 shows the reduction potentials of free and CB[7] complexed guests **1**−**5** and **1a**−**3a**. Upon inclusion within

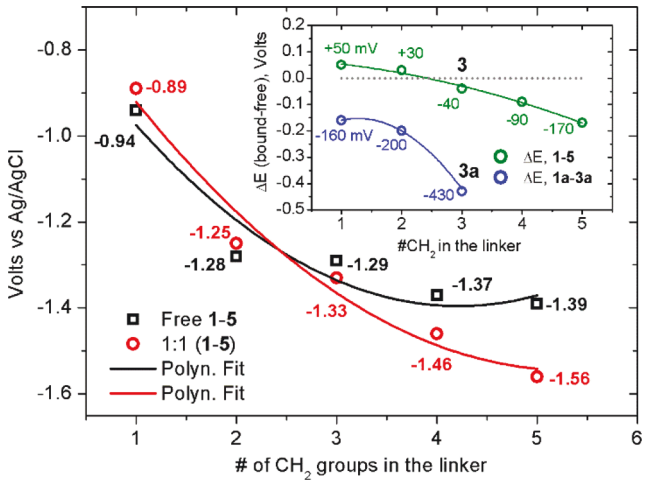

Figure 6. Reduction potentials (volts) of free **1**−**5** (E_1 for **1**, **2**) (black) and their 1:1 CB[7] complexes (red) vs linker length. Inset: ΔE (bound, free, mV) for **1**−**5** (green), **1a**−**3a** (blue). E_1 used for **1**, **2**, **1a**, and **2a**. Fit applied to aid in visualization.

CB[7], **1** and **2** showed a small positive shift of the reduction potential which could be due to the low polarizability and electron density of the CB[7] inner cavity.[40,41] Upon increasing the linker length (**3**−**5**), a gradual negative shift is observed. This is consistent with binding modes observed by NMR titration and QC calculations discussed above. Extension of the hydrophobic linker leads to its placement in the inner cavity, while positive charges of pyridinium rings move closer to electron-rich portals. Favorable ion−dipole interaction between the portals of CB and the guest positive charges "shields" the electron acceptor pyridinium rings and leads to the negative shift of their reduction potential.[42]

Compounds **1a**−**3a** displayed much larger negative shifts than **1**−**3**. This is consistent with the stronger binding as noted from the NMR and ITC data. In these cases, for a given linker length, positive charges are located closer to carbonyl rims than in **1**−**3**. This result is best illustrated by comparing **3** and **3a** (Figure 7). While **3** exhibited a small shift of −40 mV, **3a** showed the largest shift among all studied compounds of −430 mV. Since the reduction potential of **3a** with CB[7] falls outside the electrochemical window of water, we performed the measurements in nonaqueous media. Reliability of comparison between H_2O and DMSO solutions is illustrated in Figure 7 (A vs B, also Figures S41−43 and S47−50).

A final note relates to the formation of a 2:1 complex of **5** with CB[7]. Cyclic voltammetry suggested the formation of a 2:1 complex (see Figure S45) in addition to a 1:1 complex. In the presence of excess CB[7], additional reduction (−1.23 V) was observed. This is consistent with the NMR titration spectra shown in Figures S15−S17. However, ITC data did not reveal the presence of the 2:1 complex (Figure S33). The difference in binding stoichiometries deduced from NMR and ITC could be due to the different concentrations required for

DOI: 10.1021/acs.joc.9b01049
J. Org. Chem. 2019, 84, 8759−8765

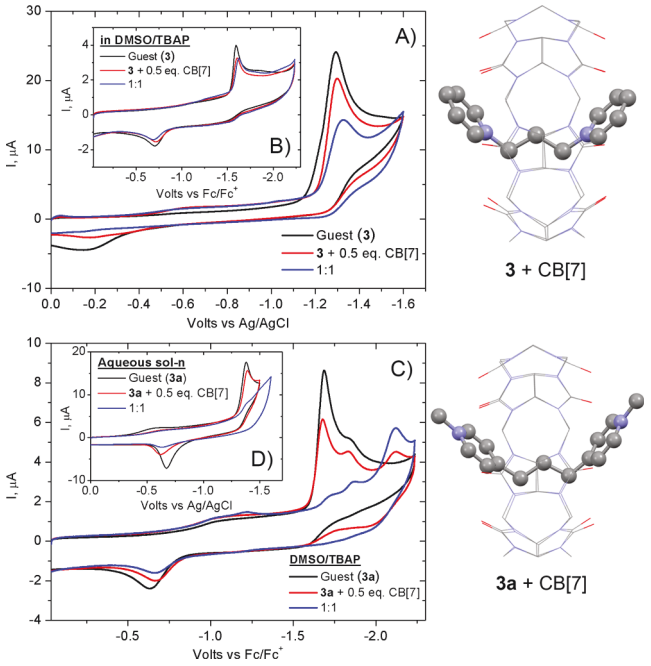

Figure 7. Voltammograms of free guests (black), 1:2 (red; 2× excess of guest), and 1:1 (blue) complex of **3** and **3a** with CB[7] in aqueous (A, D) and nonaqueous media (B,C); computationally generated structures of 1:1 complexes of **3** and **3a** with CB[7].

these experiments. In addition, the limitations of the ITC software hindered the analysis of the ITC curve with two exponentials, and we did our best to fit the curve into a single exponential. Except for **5**, no other guests showed the presence of a 2:1 complex.

In conclusion, we investigated CB[7] encapsulation of two series of bis(pyridinium)alkane dications and its effects on the electron-accepting ability of pyridinium units. Our studies bring out the importance of the linker length and the position of nitrogen atoms in aromatic rings on the reduction potential of CB[7] complexes. The difference in electrochemical responses of two types of hosts (internal vs external N positioning) despite the same length of the linker provided specific insights into the structural sensitivity of the CB[7] complexation. We demonstrated that the reduction potentials of pyridinium salts can be noncovalently manipulated over a wide range of values by means of supramolecular chemistry. Conclusions drawn here could find potential applications in the supramolecular control of the electron-acceptor ability of organic molecules in catalytic and electron-transfer reactions.

EXPERIMENTAL SECTION

General Information. All commercially available materials were used as supplied without further purification, unless otherwise noted. Proton and carbon NMR characterization and NMR titration studies of **1**−**5** and **1a**−**3a** were performed on a Bruker Avance 500 spectrometer equipped with a cryoprobe. Chemical shifts are reported in parts per million (ppm). Deuterated solvent was used as a lock, and residual protiated solvent peak was used as reference. FIDs are available upon request. UV−vis spectra were recorded in a 1 cm Starna Cells cuvette on an Agilent 8453 UV−vis spectrometer. Mass spectrometry characterization of **1**−**5** and **1a**−**3a** was performed using a Thermo Scientific LTQ-FT, a hybrid mass spectrometer consisting of a linear ion trap (the LTQ portion), and a Fourier transform ion cyclotron resonance mass spectrometer, FT-ICR. IR spectra were recorded on a Thermo Scientific Nicolet iS5 ATR IR spectrometer. ITC measurements were performed on a Nano ITC Standard volume instrument (TA). Cyclic voltammograms were recorded on an Epsilon potentiostat/galvanostat (BASi).

^{1}H NMR Titration. Typical procedure: A 1 mM solution of CB[7] was dissolved in D_2O, and to this was added 30 mM of guest stock solution stepwise. After each addition, the NMR spectrum was collected to monitor the changes of the host and guest proton resonances.

Isothermal Scanning Calorimetry. The formation constants and thermodynamic parameters for the inclusion of bis(pyridinium)-alkane guests in CB[7] were determined by titration calorimetry using a Nano ITC standard volume instrument from TA. All solutions were prepared in purified water (Milli-Q, Millipore). A solution (0.1 mM) of bis(pyridinium)alkane guest was placed in the sample cell. As a 1 mM solution of CB[7] was added in a series of 25−40 injections (5−10 μL), the heat evolved was recorded at 25 °C. The heat of dilution was corrected by injecting the bis(pyridinium)alkane guests solution into deionized water and subtracting these data from those of the host−guest titration. Data were analyzed and fitted in the Nano-Analyze software.

Cyclic Voltammetry. To 4 mL of distilled water was added 23 mg of NaCl (anhydrous, ACS Reagent, ≥99%) to achieve 0.1 M concentration of the supporting electrolyte (0.1 M TBAP (tetrabutylammonium perchlorate, Sigma-Aldrich, for electrochemical analysis, ≥99.0%) in dry DMSO was used for nonaqueous systems). A solution was transferred to a single-compartment glass electrochemical cell equipped with a Teflon cap (3 electrode setup) and a nitrogen inlet Teflon tube. Typically, the cell was fitted with a glassy carbon (GC) working electrode, Pt wire auxiliary electrode, and Ag/AgCl reference electrode (Ag/$AgNO_3$ for nonaqueous solutions, the Fc/Fc^+ redox couple was used as an internal standard). Nitrogen was bubbled through the solution for 20 min to remove the dissolved oxygen. During the measurements, the Teflon tube was removed from the solution and kept above the liquid to prevent oxygen from redissolving.

The working electrode was polished on a microcloth using polishing alumina. The electrode was sonicated in deionized water to remove any alumina left after polishing, rinsed with distilled water, and dried using a KimWipe. The electrode was polished before each measurement.

Baseline was measured in the 0-(−1600 mV) and 0-(−1800 mV) regions to ensure that no oxygen or other impurities were present in the solution.

Solid pyridinium salt was added to the above solution to achieve 0.7 mM (or 0.45 mM for less soluble compounds) concentration of a solute. The solution was sonicated for 10 s to aid in dissolving. Tetrafluoroborate salts were used for CV measurements.

The solution was further purged with nitrogen for 10 min.

Reduction peaks were recorded in the 0-(−1600 mV) or 0-(−1800 mV) regions at 100 mV/s.

To the above solution was added solid CB[7] to achieve the desired ratio (2:1 or 1:1 host−guest complexes).

After every CB[7] addition, the solution was sonicated for 10 s and purged for 10 min with nitrogen.

Reduction peaks were recorded in 0-(−1600 mV) or 0-(−1800 mV) regions at 100 mV/s.

Additional CB[7] was added to a solution of 1:1 H−G complex, and reduction peaks were recorded in 0-(−1600 mV) or 0-(−1800 mV) regions to ensure that presence of excessive amount of host molecule does not change the electrochemical response with respect to the 1:1 complex.

Computational Chemistry. Geometry optimization of individual hosts/guest and their inclusion complexes were performed using Gaussian '09 software on a Windows desktop computer.[43] Coordinates for CB[7] were imported from the crystal structure of the compound (CIF file) as a PDB file, which is usable in Gaussian '09; the structures of guests were constructed in the software. Geometry optimizations of complexes were performed individually, and the inclusion complexes were assembled using the optimized coordinates. Semiempirical calculations were performed first (SE-

DOI: 10.1021/acs.joc.9b01049
J. Org. Chem. 2019, 84, 8759−8765

PM6), and the optimized structures were then used for performing the calculations at the HF/3-21G level in the gas phase. IR frequency calculations were performed on the optimized structures, and the vibrations were confirmed to be all positive values, thereby validating the ground-state structures.

Synthesis. Compound **1a** was synthesized according to the previously reported procedure.[28] The optimized synthetic procedure has been used to prepare CB[7].[1−3]

To exchange counterions to the tetrafluoroborate, aqueous solutions of **1**−**5** and **1a**−**3a** were treated with 2 equiv of aqueous $AgBF_4$. Silver halide precipitate was filtered, and the filtrate concentrated under reduced pressure to afford tetrafluoroborate salts.

*1,1-Bis(pyridinium)methane Iodide (**1**).* To a solution of diiodomethane (Sigma-Aldrich, 99%, 52 mg, 0.2 mmol) in 5 mL of acetonitrile was added an excess of pyridine (Sigma-Aldrich, 99.8%, anhydrous, 64 mg, 0.8 mmol). The stirred solution was refluxed overnight. After being cooled to room temperature, the precipitate was filtered, washed with 1 mL of acetonitrile followed by 3 × 5 mL diethyl ether, and dried in vacuo to afford **1** as yellow powder (20 mg, 23%). Mp = 227−230 °C dec. ^{1}H NMR (500 MHz, D_2O): δ 9.22 (d, 4H, J = 5.55 Hz), 8.72 (t, 2H, J = 7.89 Hz), 8.19 (t, 4H, J = 7.02 Hz), 7.31 (s, 2H). $^{13}C\{^1H\}$ NMR (125 MHz, D_2O): δ 149.8, 145.1, 129.5, 78.0. IR (ν = cm^{-1}): 3472, 3430, 3023, 2999, 1622, 1489, 1293, 765, 687. HRMS (ESI): calcd for $C_{11}H_{12}N_2BF_4^+$ $[M - BF_4]^+$ 259.1024, found 259.1024.

*1,2-Bis(pyridinium)ethane Bromide (**2**).* Using the procedure given for the preparation of **1**, 1,2-dibromoethane (Sigma-Aldrich, 98%, 37 mg, 0.2 mmol) was reacted with pyridine (64 mg, 0.8 mmol) to afford **2** as a light yellow powder (25 mg, 36%). Mp = 278−280 °C dec. ^{1}H NMR (500 MHz, D_2O): δ 8.73 (d, 4H, J = 5.48 Hz), 8.58 (t, 2H, J = 7.89 Hz), 8.03 (t, 4H, J = 6.76 Hz), 5.24 (s, 4H). $^{13}C\{^1H\}$ NMR (125 MHz, D_2O): δ 147.5, 144.6, 129.1, 60.1. IR (ν = cm^{-1}): 3022, 2996, 2942, 1633, 1487, 1194, 775, 677. HRMS (ESI): calcd for $C_{12}H_{14}N_2BF_4^+$ $[M - BF_4]^+$ 273.1181, found 273.1180.

*1,3-Bis(pyridinium)propane Iodide (**3**).* Using the procedure given for the preparation of **1**, 1,3-diodopropane (Sigma-Aldrich, 99%, 29 mg, 0.1 mmol) was reacted with pyridine (32 mg, 0.4 mmol) to afford **3** as an off-white powder (41 mg, 92%). Mp = 197−200 °C dec. ^{1}H NMR (500 MHz, D_2O): δ 8.80 (d, 4H, J = 5.60 Hz), 8.49 (t, 2H, J = 7.87 Hz), 8.01 (t, 4H, 6.86 Hz), 2.71 (quint, J = 7.72 Hz). $^{13}C\{^1H\}$ NMR (125 MHz, D_2O): δ 146.3, 144.3, 128.6, 58.0, 31.7. IR (ν = cm^{-1}): 3027, 3007, 1631, 1479, 1170, 773, 677. HRMS (ESI): calcd for $C_{13}H_{16}N_2BF_4^+$ $[M - BF_4]^+$ 287.1337, found 287.1337.

*1,4-Bis(pyridinium)butane Iodide (**4**).* Using the procedure given for the preparation of **1**, 1,4-diodobutane (Sigma-Aldrich, ≥ 99%, 31 mg, 0.1 mmol) was reacted with pyridine (32 mg, 0.4 mmol) to afford **4** as an off-white powder (44 mg, 94%). Mp = 191−195 °C dec. ^{1}H NMR (500 MHz, D_2O): δ 8.73 (d, 4H, J = 5.79 Hz), 8.45 (t, 2H, J = 7.82 Hz), 7.97 (t, 4H, J = 6.95 Hz), 4.57 (m, 4H), 2.57 (m, 4H). $^{13}C\{^1H\}$ NMR (125 MHz, D_2O): δ 145.9, 144.1, 128.3, 60.7, 27.2. IR (ν = cm^{-1}): 3046, 1627, 1479, 1447, 1146, 817, 763. HRMS (ESI): calcd for $C_{14}H_{18}N_2I^+$ $[M - I]^+$ 341.0509, found 341,0509.

*1,5-Bis(pyridinium)pentane Iodide (**5**).* Using the procedure given for the preparation of **1**, 1,5-diodopentane (Sigma-Aldrich, 97%, 32 mg, 0.1 mmol) was reacted with pyridine (32 mg, 0.4 mmol) to afford **5** as a pale yellow powder (45 mg, 94%). Mp = 128−130 °C dec. ^{1}H NMR (500 MHz, D_2O): δ 8.72 (d, 4H, J = 5.58 Hz), 8.44 (t, 2H, J = 7.86 Hz), 7.96 (t, 4H, J = 6.97 Hz), 4.51 (t, 4H, J = 7.45 Hz), 1.98 (quint, 4H, J = 7.66 Hz), 1.32 (quint, 2H, J = 7.80 Hz). $^{13}C\{^1H\}$ NMR (125 MHz, D_2O): δ 145.6, 144.1, 128.2, 61.3, 29.9, 22.0. IR (ν = cm^{-1}): 3420, 3377, 3011, 1629, 1489, 1234, 1163, 775, 683. HRMS (ESI): calcd for $C_{15}H_{20}N_2I^+$ $[M - I]^+$ 355.0666, found 355.0665.

*1,2-Bis(N-methylpyridin-4-ium)ethane Iodide (**2a**).* To a solution of 1,2-bis(4-pyridyl)ethane (Sigma-Aldrich, 99%, 36 mg, 0.2 mmol) in 5 mL of acetonitrile was added an excess of methyl iodide (240 mg, 1.6 mmol), and the stirred reaction mixture was refluxed overnight. After being cooled to room temperature, the precipitate was filtered, washed with 0.5 mL of acetonitrile and 2 × 5 mL of diethyl ether, and dried in vacuo to afford **2a** as a cream-colored powder (78 mg, 84%). Mp = 127−130 °C dec. ^{1}H NMR (500 MHz, D_2O): δ 8.53 (d, 4H, J = 6.63 Hz), 7.77 (d, 4H, J = 6.55 Hz), 4.21 (s, 6H), 3.28 (s, 4H). $^{13}C\{^1H\}$ NMR (125 MHz, D_2O): δ 159.96, 144.55, 127.66, 47.37, 34.00. IR (BF_4^- salt, ν = cm^{-1}): 3066, 1647, 1479, 1191, 1021, 848, 814, 575. HRMS (ESI): calcd for $C_{14}H_{18}N_2BF_4^+$ $[M - BF_4]^+$ 301.1494, found 301.1493.

*1,3-Bis(N-methylpyridin-4-ium)propane Iodide (**3a**).* Using the procedure given for the preparation of **2a**, 4,4′-trimethylenepyridine (Sigma-Aldrich, 98%, 39 mg, 0.2 mmol) was reacted with an excess of methyl iodide (240 mg, 1.6 mmol). To aid in the precipitation, after being cooled to room temperature, the reaction mixture was concentrated under reduced pressure until the precipitate formed. Following the same steps after the filtration as described for **2a**, we obtained **3a** as an off-white powder (78 mg, 51%). Mp = >300 °C dec. ^{1}H NMR (500 MHz, D_2O): δ 8.51 (d, 4H, J = 6.60 Hz), 7.77 (d, 4H, J = 6.42 Hz), 4.20 (s, 6H), 2,89 (t, 4H, J = 7.75 Hz), 2.06 (quint, 2H, J = 7.84 Hz). $^{13}C\{^1H\}$ NMR (125 MHz, D_2O): δ 161.86, 144.29, 127.58, 47.24, 34.10, 28.42. IR (BF_4^- salt, ν = cm^{-1}): 3284, 3110, 1645, 1519, 1476, 1287, 1028, 835. HRMS (ESI): calcd for $C_{15}H_{20}N_2BF_4^+$ $[M - BF_4]^+$ 315.1650, found 315.1650.

■ ASSOCIATED CONTENT

Supporting Information

The Supporting Information is available free of charge on the ACS Publications website at DOI: 10.1021/acs.joc.9b01049.

NMR and ITC titration data, cyclic voltammetry data, scan rate experiments, quantum chemical calculations, Cartesian coordinates (PDF)

■ AUTHOR INFORMATION

Corresponding Authors

*E-mail: pattabiraman2@unk.edu.
*E-mail: murthy1@miami.edu.
*E-mail: rmw@bgsu.edu.

ORCID

Vaidhyanathan Ramamurthy: 0000-0002-3168-2185
R. Marshall Wilson: 0000-0003-2294-0936

Notes

The authors declare no competing financial interest.

■ ACKNOWLEDGMENTS

R.M.W. thanks the R. Marshall and Antonia G. Wilson Chemistry Fund for financial support of this research. V.R. thanks the National Science Foundation (CHE-1807729) for financial support. Research activity at UNK was supported by Great Plains IDeA-CTR Pilot Grant (NIGMS 1U54GM115458-01). N.A.T. and A.A.T. thank Stefan Ilic (UIC) and Dr. Stephania Messersmith (BGSU) for CV training. R.M.W. thanks Dr. Larry Sallans (UC) for the mass spectral analysis.

■ REFERENCES

(1) Behrend, R.; Meyer, E.; Rusche, F. Ueber Condensationsproducte aus Glycoluril und Formaldehyd. *Liebigs Annalen der Chemie* **1905**, *339*, 1−37.

(2) Freeman, W. A.; Mock, W. L.; Shih, N.-Y. Cucurbituril. *J. Am. Chem. Soc.* **1981**, *103*, 7367−7368.

(3) Kim, J.; Jung, I.-S.; Kim, S.-Y.; Lee, E.; Kang, J.-K.; Sakamoto, S.; Yamaguchi, K.; Kim, K. New Cucurbituril Homologues: Syntheses, Isolation, Characterization, and X-ray Crystal Structures of Cucurbit[n]uril (n = 5, 7, and 8). *J. Am. Chem. Soc.* **2000**, *122*, 540−541.

(4) Jeon, W. S.; Ziganshina, A. Y.; Lee, J. W.; Ko, Y. H.; Kang, J.-K.; Lee, C.; Kim, K. A [2]Pseudorotaxane Based Molecular Machine: Reversible Formation of a Molecular Loop Driven by Electrochemical

DOI: 10.1021/acs.joc.9b01049
J. Org. Chem. 2019, 84, 8759−8765

and Photochemical Stimuli. *Angew. Chem., Int. Ed.* **2003**, *42*, 4097−4100.
(5) Kim, K.; Selvapalam, N.; Oh, D. H. Cucurbiturils-a New Family of Host Molecules. *J. Incl. Macrocycl. Chem.* **2004**, *50*, 31−36.
(6) Barrow, S. J.; Kasera, S.; Rowland, M. J.; Barrio, J.; Scherman, O. A. Cucurbituril-Based Molecular Recognition. *Chem. Rev.* **2015**, *115*, 12320−12406.
(7) Lagona, J.; Mukhopadhyay, P.; Chakrabarti, S.; Isaacs, L. The Cucurbit[*n*]uril Family. *Angew. Chem., Int. Ed.* **2005**, *44*, 4844−4870.
(8) Masson, E.; Ling, X.; Roymon, J.; Mensah-Kyermeh, L.; Lu, X. Cucurbituril Chemistry: A Tale of Supramolecular Success. *RSC Adv.* **2012**, *2*, 1213−1247.
(9) Assaf, K. I.; Nau, W. M. Cucurbiturils: From Synthesis to High-Affinity Binding and Catalysis. *Chem. Soc. Rev.* **2015**, *44*, 394−418.
(10) Pattabiraman, M.; Natarajan, A.; Kaanumalle, L.; Ramamurthy, V. Templating Photodimerization of *trans*-Cinnamic Acids with Cucurbit[8]uril and γ-Cyclodextrin. *Org. Lett.* **2005**, *7*, 529−532.
(11) Pemberton, B. C.; Barooah, N.; Srivatsava, D. K.; Sivaguru, J. Supramolecular Photocatalysis by Confinement-Photodimerization of Coumarins Within Cucurbit[8]urils. *Chem. Commun.* **2010**, *46*, 225−227.
(12) Hettiarachchi, G.; Nguyen, D.; Wu, J.; Lucas, D.; Ma, D.; Isaacs, L.; Briken, V. Toxicology and Drug Delivery by Cucurbit[n]-uril Type Molecular Containers. *PLoS One* **2010**, *5*, No. e10514.
(13) Coti, K. K.; Belowich, M.; Liong, M.; Ambrogio, M. W.; Lau, Y. A.; Hussam, A. K.; Zink, J. I.; Khashab, N. M.; Stoddart, J. F. Mechanised Nanoparticles for Drug Delivery. *Nanoscale* **2009**, *1*, 16−39.
(14) Ben Shir, I. B.; Sasmal, S.; Mejuch, T.; Sinha, M. K.; Kapon, M.; Keinan, E. Repulsive Interaction Can Be a Key Design Element of Molecular Rotary Motors. *J. Org. Chem.* **2008**, *73*, 8772−8779.
(15) Zhu, L.; Yan, H.; Wang, X.-J.; Zhao, Y. Light-Controllable Cucurbit[7]uril-Based Molecular Shuttle. *J. Org. Chem.* **2012**, *77*, 10168−10175.
(16) Ong, W.; Gomez-Kaifer, M.; Kaifer, A. E. Cucurbit[7]uril: A Very Effective Host for Viologens and Their Cation Radicals. *Org. Lett.* **2002**, *4*, 1791−1794.
(17) Kim, H.-J.; Jeon, W. S.; Ko, Y. H.; Kim, K. Inclusion of Methylviologen in Cucurbit[7]uril. *Proc. Natl. Acad. Sci. U. S. A.* **2002**, *99*, 5007−5011.
(18) Moon, K.; Kaifer, A. E. Modes of Binding Interaction between Viologen Guests and the Cucurbit[7]uril Host. *Org. Lett.* **2004**, *6*, 185−188.
(19) Yuan, L.; Wang, R.; Macartney, D. Binding Modes of Cucurbit[6]uril and Cucurbit[7]uril with a Tetracationic Bis-(viologen) Guest. *J. Org. Chem.* **2007**, *72*, 4539−4542.
(20) Freitag, M.; Gundlach, L.; Piotrowiak, P.; Galoppini, E. Fluorescence Enhancement of Di-p-tolyl Viologen by Complexation in Cucurbit[7]uril. *J. Am. Chem. Soc.* **2012**, *134*, 3358−3366.
(21) Gong, W.; Yang, X.; Zavalij, P. Y.; Isaacs, L.; Zhao, Z.; Liu, S. From Packed "Sandwich"to "Russian Doll": Assembly by Charge-Transfer Interactions in Cucurbit[10]uril. *Chem. - Eur. J.* **2016**, *22*, 17612−17618.
(22) Wyman, I. W.; Macartney, D. H. Cucurbit[7]uril Host-guest and Pseudorotaxane Complexes with α,ω-bis(pyridinium)alkane Dications. *Org. Biomol. Chem.* **2009**, *7*, 4045−4051.
(23) Gamal-Eldin, M. A.; Macartney, D. H. Cucurbit[7]uril Host-guest Complexes and [2]pseudorotaxanes with *N*-methylpiperidinium, *N*-methylpyrrolidinium, and *N*-methylmorpholinium Cations in Aqueous Solution. *Org. Biomol. Chem.* **2013**, *11*, 1234−1241.
(24) Li, S.; Miao, X.; Wyman, I. W.; Li, Y.; Zheng, Y.; Wang, Y.; Macartney, D. H.; Wang, R. High-affinity Host-guest Complex of Cucurbit[7]uril with a Bis(thiazolium) Salt. *RSC Adv.* **2015**, *5*, 56110−56115.
(25) Nagamura, T.; Kashihara, S.; Kawai, H. First Intramolecular Charge Resonance Band Observed at Room Temperature in Solution by Steady Photolysis of 1,3-bis(4-(4-nitrostyryl)pyridinium)propane Tetraphenylborate. *Chem. Phys. Lett.* **1998**, *294*, 167−172.
(26) Pernak, J.; Rogoża, J.; Mirska, I. Synthesis and Antimicrobial Activities of New Pyridinium and Benzimidazolium Chlorides. *Eur. J. Med. Chem.* **2001**, *36*, 313−320.
(27) Alptüzün, V.; Parlar, S.; Taşlı, H.; Erciyas, E. Synthesis and Antimicrobial Activity of Some Pyridinium Salts. *Molecules* **2009**, *14*, 5203−5215.
(28) Tikhomirova, A. A.; Tcyrulnikov, N. A.; Wilson, R. M. Aerobic Oxidation of in Situ Generated Cyanine Dyes Leading to DNA Damage. *Org. Lett.* **2019**, *21*, 1449−1452.
(29) He, S.; Zhou, C.; Zhang, H.; Zhou, X. Binding Modes of Cucurbit[6]uril and Cucurbit[7]uril with a Series of Bis-pyridinium Compounds. *J. Inclusion Phenom. Macrocyclic Chem.* **2013**, *76*, 333−344.
(30) Wang, J.; *Analytical Electrochemistry*, 3rd ed.; John Wiley & Sons: Hoboken, NJ, 2006.
(31) Gaudiello, J. G.; Larkin, D.; Rawn, J. D.; Sosnowki, J. J. On the Mechanism of the Electrochemical Reduction of *N*-methylpyridinium Ion. *J. Electroanal. Chem.* **1982**, *131*, 203−214.
(32) Hermolin, J.; Kosower, E. M. Stable Free Radicals. 12. New Aspects of the Behavior of 1-alkyl-4-(carboalkoxy)- and 1-alkyl-4-carbamidopyridinyl Radicals in Solution and in Thin Films. *J. Am. Chem. Soc.* **1981**, *103*, 4808−4813.
(33) Ikegami, Y.; Muramatsu, T.; Hanaya, K.; Onodera, S.; Nakayama, N.; Kosower, E. M. The 1,1′-ethylenebis[4-(methoxycarbonyl)pyridinyl] Diradical and its Photosensitive Cyclomers. *J. Am. Chem. Soc.* **1987**, *109*, 2876−2880.
(34) Muramatsu, T.; Toyota, A.; Suzuki, M. Visible Light Sensitive Cyclomer and Its Tautomeric Dispiro Compound Formed from Bispyridinyl Diradical. *J. Am. Chem. Soc.* **2005**, *127*, 4572−4573.
(35) Sindelar, V.; Silvi, S.; Parker, S. E.; Sobransingh, S.; Kaifer, A. E. Proton and Electron Transfer Control of the Position of Cucurbit-[n]uril Wheels in Pseudorotaxanes. *Adv. Funct. Mater.* **2007**, *17*, 694−701.
(36) Park, S. H.; Kawai, H.; Nagamura, T. First Observation of Monomer and Dimer Radical Cation upon Photoreduction of Cyanopyridinium Derivatives in Solution by Electron Spin Resonance and Absorption Spectroscopy. *J. Phys. Chem. A* **2002**, *106*, 11987−11991.
(37) Kahlfuss, C.; Saint-Aman, E.; Bucher, C. Redox-controlled Intramolecular Motions Triggered by π-dimerization and Primerization Processes. In *Organic Redox Systems*; Nishinaga, T., Ed.; John Wiley & Sons: Hoboken, NJ, 2006; pp 49−50.
(38) Kato, S.-I.; Matsumoto, T.; Ideta, K.; Shimasaki, T.; Goto, K.; Shinmyozu, T. Supramolecular Assemblies and Redox Modulation of Pyromellitic Diimide-Based Cyclophane via Noncovalent Interactions with Naphthol. *J. Org. Chem.* **2006**, *71*, 4723−4733.
(39) Lebègue, E.; Agullo, J.; Bélanger, D. Electrochemical Behavior of Pyridinium and *N*-Methyl Pyridinium Cations in Aqueous Electrolytes for CO_2 Reduction. *ChemSusChem* **2018**, *11*, 219−228.
(40) Nau, W. M.; Florea, M.; Assaf, K. I. Deep Inside Cucurbiturils: Physical Properties and Volumes of their Inner Cavity Determine the Hydrophobic Driving Force for Host-Guest Complexation. *Isr. J. Chem.* **2011**, *51*, 559−577.
(41) Dsouza, R. N.; Pischel, U.; Nau, W. M. Complexation of Fluorescent Dyes by Macrocyclic Hosts. In *Supramolecular Photochemistry: Controlling Photochemical Processes*; Ramamurthy, V., Inoue, Y., Ed.; John Wiley & Sons: Hoboken, NJ, 2011, 100.
(42) Song, Q.; Li, F.; Wang, Z.; Zhang, X. A Supramolecular Strategy for Tuning the Energy Level of Naphthalenediimide: Promoted Formation of Radical Anions with Extraordinary Stability. *Chem. Sci.* **2015**, *6*, 3342−3346.
(43) *Gaussian 09*, Revision D.01; Frisch, M. J.; Trucks, G. W.; Schlegel, H. B.; Scuseria, G. E.; Robb, M. A.; Cheeseman, J. R.; Scalmani, G.; Barone, V.; Mennucci, B.; Petersson, G. A.; Nakatsuji, H.; Caricato, M.; Li, X.; Hratchian, H. P.; Izmaylov, A. F.; Bloino, J.; Zheng, G.; Sonnenberg, J. L.; Hada, M.; Ehara, M.; Toyota, K.; Fukuda, R.; Hasegawa, J.; Ishida, M.; Nakajima, T.; Honda, Y.; Kitao, O.; Nakai, H.; Vreven, T.; Montgomery, J. A., Jr.; Peralta, J. E.; Ogliaro, F.; Bearpark, M.; Heyd, J. J.; Brothers, E.; Kudin, K. N.;

DOI: 10.1021/acs.joc.9b01049
J. Org. Chem. 2019, 84, 8759−8765

Staroverov, V. N.; Keith, T.; Kobayashi, R.; Normand, J.; Raghavachari, K.; Rendell, A.; Burant, J. C.; Iyengar, S. S.; Tomasi, J.; Cossi, M.; Rega, N.; Millam, J. M.; Klene, M.; Knox, J. E.; Cross, J. B.; Bakken, V.; Adamo, C.; Jaramillo, J.; Gomperts, R.; Stratmann, R. E.; Yazyev, O.; Austin, A. J.; Cammi, R.; Pomelli, C.; Ochterski, J. W.; Martin, R. L.; Morokuma, K.; Zakrzewski, V. G.; Voth, G. A.; Salvador, P.; Dannenberg, J. J.; Dapprich, S.; Daniels, A. D.; Farkas, O.; Foresman, J. B.; Ortiz, J. V.; Cioslowski, J.; Fox, D. J., Gaussian, Inc., Wallingford CT, 2013.

DOI: 10.1021/acs.joc.9b01049
J. Org. Chem. 2019, 84, 8759−8765